

Alfvén eigenmodes in cylindrical geometry

This report discusses Alfvén eigenmodes in cylindrical plasmas. Gauss units system is adopted in this note.

1 Eigenmode equation

The eigenmode equation given by Huishan takes the following form:

$$\frac{d}{dr} \left[A(r, \omega) \frac{d}{dr} (r \delta \xi_r) \right] - C(r, \omega) r \delta \xi_r = 0, \quad (1)$$

where the coefficients $A(r, \omega)$ and $C(r, \omega)$ are given by

$$A(r, \omega) = \frac{1}{D} \frac{\rho}{r} (C_s^2 + V_A^2) (\omega^2 - \omega_a^2) (\omega^2 - \omega_h^2) \quad (2)$$

$$C(r, \omega) = \frac{1}{4\pi} \frac{d}{dr} \left(\frac{B_\theta^2}{r^2} \right) + \frac{1}{2\pi} \frac{d}{dr} \left[\frac{n B_\theta}{r^2} \frac{G}{R} \frac{1}{D} (\omega^2 - \omega_h^2) (C_s^2 + V_A^2) \right] + \frac{1}{\pi} \frac{1}{D} \frac{n^2 B_\theta^2 V_A^2}{r^3 R^2} (\omega^2 - \omega_g^2) - (\omega^2 - \omega_a^2) \frac{\rho}{r}, \quad (3)$$

where V_A and C_s are respectively Alfvén speed and acoustic speed, which are respectively given by

$$V_A = \frac{B^2}{4\pi\rho} \quad (4)$$

and

$$C_s = \frac{\gamma P}{\rho}. \quad (5)$$

The other quantities appearing in the coefficients (2) and (3) are given by

$$\omega_a^2 = \frac{F^2}{4\pi\rho}, F \equiv \frac{B_\theta}{r} (m - nq), \quad (6)$$

$$\omega_h^2 = \frac{C_s^2}{C_s^2 + V_A^2} \omega_a^2, \quad (7)$$

$$\omega_g^2 = \frac{C_s^2}{V_A^2} \omega_a^2 \quad (8)$$

$$G = \frac{m B_z}{r} + \frac{n B_\theta}{R}, \quad (9)$$

$$D = \omega^4 + k^2 C_s^2 \omega_a^2 - (C_s^2 + V_A^2) k^2 \omega^2, \quad (10)$$

and

$$k^2 = \frac{m^2}{r^2} + \frac{n^2}{R^2}. \quad (11)$$

1.1 Normalized eigenmode equation

Define

$$V_{A0}^2 \equiv \frac{B_0^2}{4\pi\rho_0} \quad (12)$$

$$\omega_{A0} \equiv \frac{V_{A0}}{a}, \quad (13)$$

where ρ_0 and B_0 are mass density and strength of magnetic field at the magnetic axis, respectively. Define $\bar{r} = r/a$, $\bar{\rho} = \rho/\rho_0$, $\bar{\omega} = \omega/\omega_{A0}$, $\bar{\omega}_a = \omega_a/\omega_{A0}$, $\bar{\omega}_h = \omega_h/\omega_{A0}$, $\bar{\omega}_g = \omega_g/\omega_{A0}$, $\bar{P}_0 = P/(B_0^2/(8\pi))$, $\bar{V}_A = V_A/V_{A0}^2$, $\bar{C}_s = C_s/V_{A0}$, $\bar{k} = ka$. Equation (1) is written as

$$\frac{d}{d\bar{r}} \left[A \frac{du}{d\bar{r}} \right] - a^2 C u = 0, \quad (14)$$

and the coefficient A is written as

$$\begin{aligned} A &= \frac{1}{D} \frac{\rho}{r} (C_s^2 + V_A^2) (\omega^2 - \omega_a^2) (\omega^2 - \omega_h^2) \\ &= \frac{1}{\bar{D}} \frac{\bar{\rho}}{\bar{r}} (\bar{C}_s^2 + \bar{V}_A^2) (\bar{\omega}^2 - \bar{\omega}_a^2) (\bar{\omega}^2 - \bar{\omega}_h^2) \left(\frac{\rho_0}{a} V_{A0}^2 \right), \end{aligned} \quad (15)$$

where

$$\begin{aligned}\bar{D} &\equiv \frac{D}{\omega_{A0}^4} \\ &= \bar{\omega}^4 + \frac{k^2 C_s^2}{\omega_{A0}^2} \bar{\omega}_a^2 - \frac{k^2 (C_s^2 + V_A^2)}{\omega_{A0}^2} \bar{\omega}^2 \\ &= \bar{\omega}^4 + \bar{k}^2 \bar{C}_s^2 \bar{\omega}_a^2 - \bar{k}^2 (\bar{C}_s^2 + \bar{V}_A^2) \bar{\omega}^2,\end{aligned}\quad (16)$$

$$\bar{k}^2 = k^2 a^2 = \frac{m^2}{\bar{r}^2} + n^2 \varepsilon_a^2 \quad (17)$$

$$\varepsilon_a \equiv \frac{a}{R} \quad (18)$$

$$\bar{V}_A^2 = \frac{V_A^2}{V_{A0}^2} = \frac{\bar{B}^2}{\bar{\rho}} \quad (19)$$

$$\bar{C}_s^2 \equiv \frac{C_s^2}{V_{A0}^2} = \frac{\gamma \bar{P}}{2 \bar{\rho}} \quad (20)$$

$$\bar{\omega}_a^2 = \frac{\omega_a^2}{\omega_{A0}^2} = \frac{\frac{F^2}{4\pi\rho}}{\frac{B_\theta^2}{4\pi\rho_0} \frac{1}{a^2}} = \frac{\frac{F^2}{\bar{\rho}} a^2}{B_0^2} = \frac{\bar{B}_\theta^2}{\bar{r}^2 \bar{\rho}} (m - nq)^2 \quad (21)$$

$$\bar{\omega}_h^2 = \frac{\omega_h^2}{\omega_{A0}^2} = \frac{\bar{C}_s^2}{\bar{C}_s^2 + \bar{V}_A^2} \bar{\omega}_a^2 \quad (22)$$

The coefficient $C(r, \omega)$ can be written as

$$C = C_1 + C_2 + C_3, \quad (23)$$

with

$$C_1 = \frac{1}{4\pi} \frac{d}{dr} \left(\frac{B_\theta^2}{r^2} \right) \quad (24)$$

$$C_2 = \frac{1}{2\pi} \frac{d}{dr} \left[\frac{n B_\theta}{r^2} \frac{G}{R} \frac{1}{D} (\omega^2 - \omega_h^2) (C_s^2 + V_A^2) \right] \quad (25)$$

$$C_3 = \frac{1}{\pi} \frac{1}{D} \frac{n^2 B_\theta^2 V_A^2}{r^3 R^2} (\omega^2 - \omega_g^2) - (\omega^2 - \omega_a^2) \frac{\rho}{r} \quad (26)$$

Then

$$\begin{aligned}a^2 C_1 &= a^2 \frac{1}{4\pi} \frac{d}{dr} \left(\frac{B_\theta^2}{r^2} \right) \\ &= \frac{d}{d\bar{r}} \left(\frac{\bar{B}_\theta^2}{\bar{r}^2} \right) \rho_0 \frac{V_{A0}^2}{a}\end{aligned}\quad (27)$$

$$\begin{aligned}a^2 C_2 &= a^2 \frac{1}{2\pi} \frac{d}{dr} \left[\frac{n B_\theta}{r^2} \frac{G}{R} \frac{1}{D} (\omega^2 - \omega_h^2) (C_s^2 + V_A^2) \right] \\ &= \frac{d}{d\bar{r}} \left[\frac{n \bar{B}_\theta}{\bar{r}^2} \bar{G} \varepsilon_a \frac{1}{\bar{D}} (\bar{\omega}^2 - \bar{\omega}_h^2) (\bar{C}_s^2 + \bar{V}_A^2) \right] 2 \left(\frac{\rho_0}{a} V_{A0}^2 \right)\end{aligned}\quad (28)$$

$$\begin{aligned}a^2 C_3 &= a^2 \frac{1}{\pi} \frac{1}{D} \frac{n^2 B_\theta^2 V_A^2}{r^3 R^2} (\omega^2 - \omega_g^2) - a^2 (\omega^2 - \omega_a^2) \frac{\rho}{r} \\ &= \frac{1}{\bar{D}} \frac{n^2 \bar{B}_\theta^2 \bar{V}_A^2}{\bar{r}^3} (\bar{\omega}^2 - \bar{\omega}_g^2) (4 \varepsilon_a^2) \left(\frac{\rho_0}{a} V_{A0}^2 \right) - (\bar{\omega}^2 - \bar{\omega}_a^2) \frac{\bar{\rho}}{\bar{r}} \left(V_{A0}^2 \frac{\rho_0}{a} \right).\end{aligned}\quad (29)$$

$$\bar{G} = \frac{m \bar{B}_z}{\bar{r}} + n \bar{B}_\theta \varepsilon_a \quad (30)$$

2 Benchmark

I developed a numerical code that solves the eigenmode equation by using the finite elements expansion method. To benchmark the code, I calculate the eigenmode structure and frequency of a simple equilibrium and compare the results we obtained with those given in Ref. [1]. The simple equilibrium is given by

$$\varepsilon_a = 1.0, \quad (31)$$

$$P = 0, \quad (32)$$

$$\rho = 1.0 - 0.98 \left(\frac{r}{a} \right)^2, \quad (33)$$

$$q = 1.001 + 2.0 \left(\frac{r}{a} \right)^2, \quad (34)$$

and the B_z is set to be constant,

$$\frac{B_z}{B_0} = 1.0. \quad (35)$$

Using the relation between B_z and B_θ , we obtain

$$B_\theta = \frac{B_z r}{q(r)R}. \quad (36)$$

The profiles of equilibrium quantities are plotted in Fig. 1.

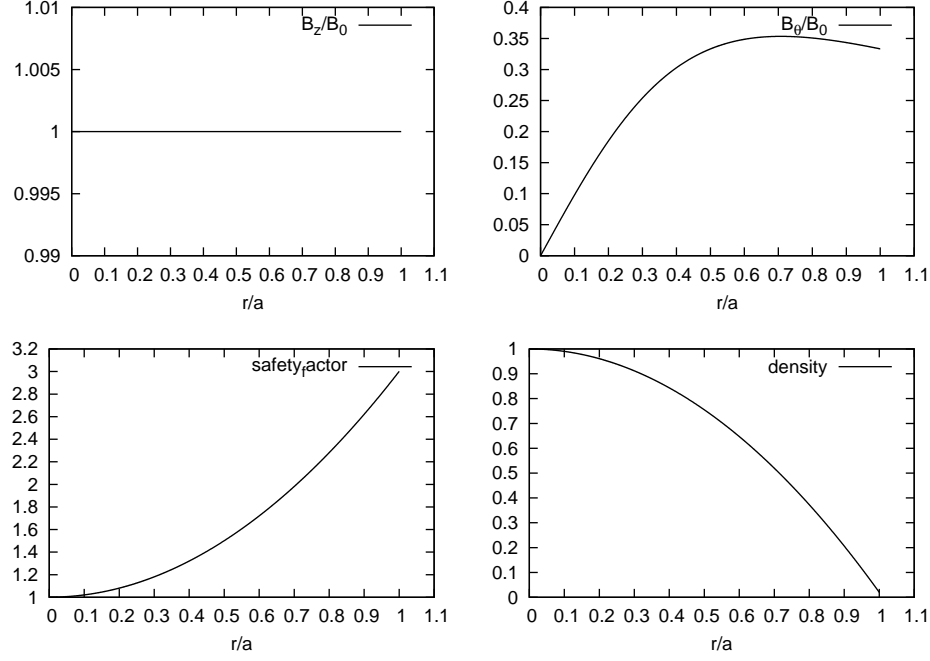


Figure 1. Profiles of equilibrium quantities

In the simple equilibrium specified above, a global ($m = 2, n = 0$) mode with frequency $\omega^2 = 1.92768$ is found. The eigenfunction and continuum are plotted in Fig. 2.

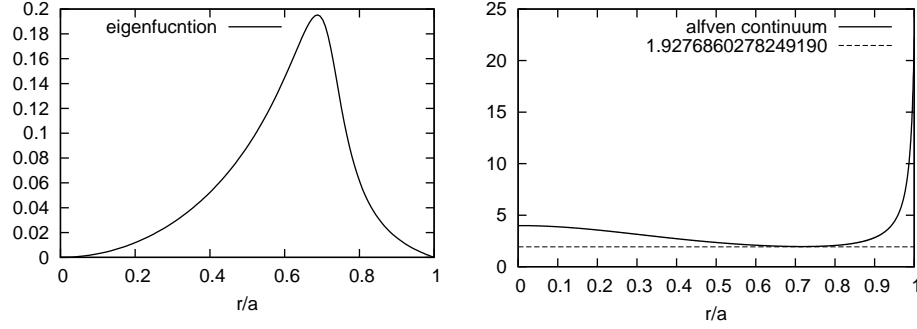


Figure 2. Left figure: Radial eigenfunction of a ($m = 2, n = 0$) mode and Right figure: Continuum with $m = 2$ and $n = 0$.

The eigenfrequency I obtained ($\omega^2 = 1.92768$) agrees roughly with the one ($\omega^2 = 1.916311$) reported in Ref. [1].

3 Analytical Reverse Field Pinch (RFP) equilibrium

$$\begin{aligned} \mathcal{E}_a &= 0.5/1.5, \quad m=1, n=4 \\ q(r) &= 0.218833 - 0.406249r^2 + 0.268598r^4 - 0.163605r^6 + 0.092078r^8 \\ p(r) &= a_0(1.037632 + 0.517353r^2 - 6.776814r^4 + 7.683398r^6 - 2.466511r^8 + 3.5e^{-r^2/0.044}) \\ \psi(r) &= 1.825021r^2 - 0.804835r^4 - 0.402203r^6 + 0.382017r^8 \\ B_z(r) &= \frac{q(r)}{r} \frac{d\psi}{dr}, \\ B_\theta(r) &= \mathcal{E}_a \frac{d\psi}{dr}, \end{aligned}$$

其中压强表达式中的参数 a 有 $\beta(r=0) = 9\%$ 来确定。

Figure 3. Analytical RFP equilibrium configuration specified by Huishan (I guess that the analytical expression is obtained by using an interpolating formula to fit the numerical results)

The profiles of the equilibrium quantities are plotted in Fig. 4

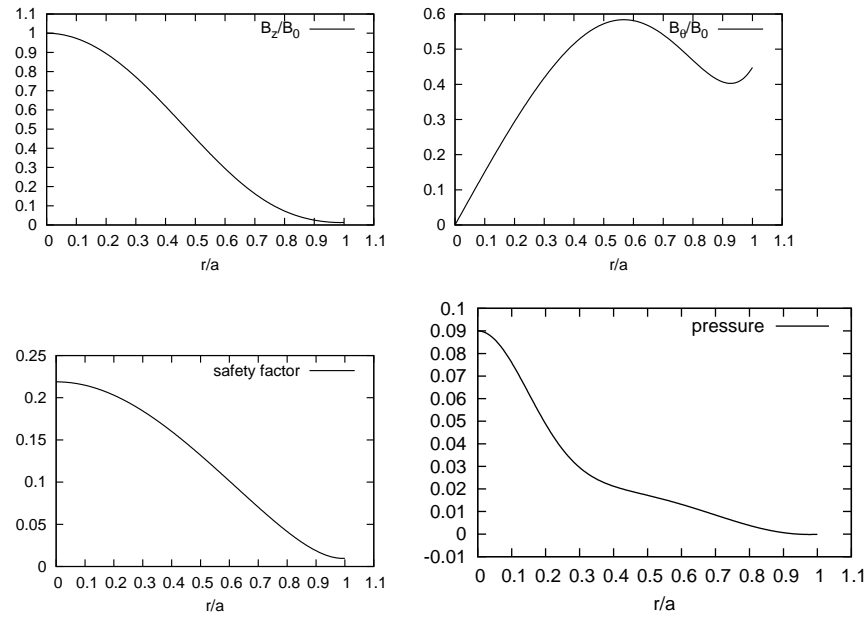


Figure 4. Profiles of RFP equilibrium quantities

For the above RFP equilibrium, we choose a uniform density profile. For this case, a global mode with frequency $\omega^2 = 1.05231 \times 10^{-2}$ is found. The eigenfunction and continuum are plotted in Fig. 5.

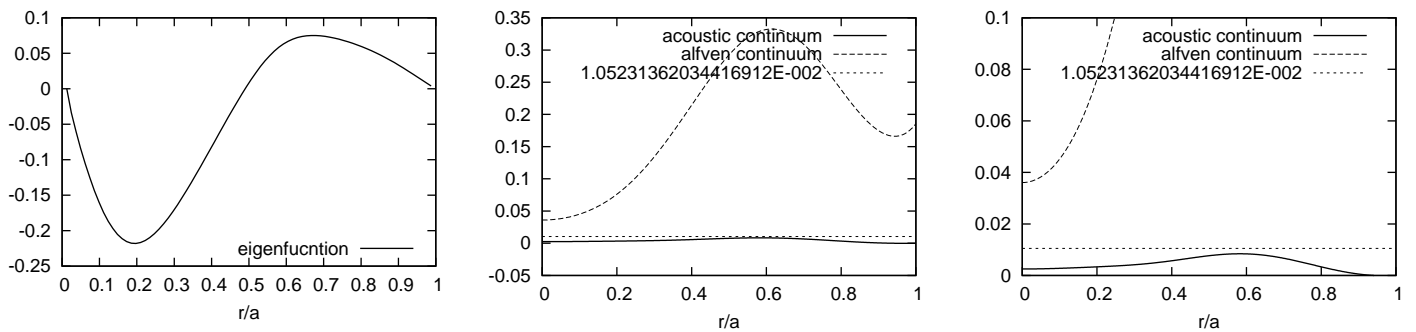


Figure 5. (a) Eigenfunction and (b) continue spectrum. The last figure is a replot of the second figure with the y-range limited to the range $[0:0.1]$ to show the details in this range.

Next we choose a RFP equilibrium with a nonuniform density profile, which is given by Eq. (33). All other profiles are the same as those in the last example. For this case, a global mode with frequency $\omega^2 = 1.4959 \times 10^{-2}$ is found. The eigenfunction and continuum are plotted in Fig. 6.

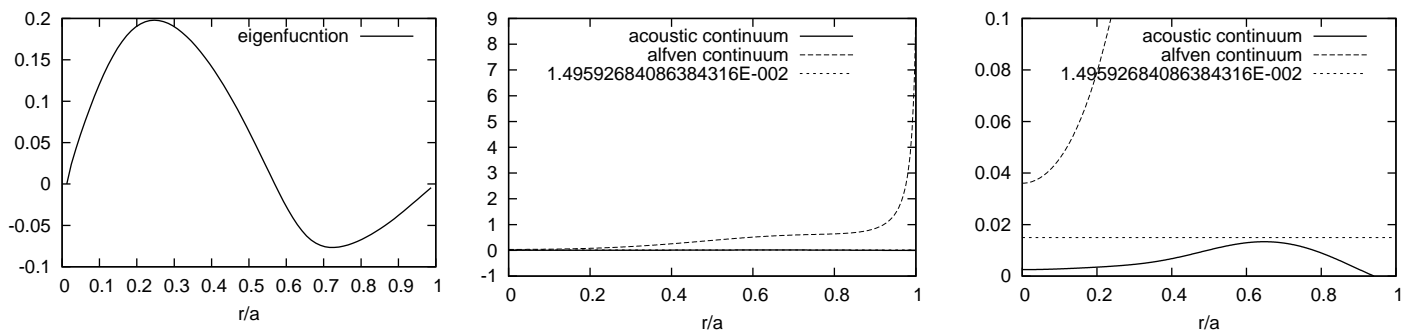


Figure 6. (a) Eigenfunction and (b) continue spectrum. The last figure is a replot of the second figure with the y-range limited to the range $[0:0.1]$ to show the details in this range.

4 Force balance in cylindrical geometry

The force balance equation is

$$\frac{4\pi}{c} \mathbf{J} \times \mathbf{B} = 4\pi \nabla P. \quad (37)$$

In cylindrical geometry, the magnetic field is assumed to take the following form

$$\mathbf{B} = B_z(r) \mathbf{e}_z + B_\theta(r) \mathbf{e}_\theta, \quad (38)$$

where (r, θ, z) is the usual cylindrical coordinates. Using Eq. (38), the current density is written as

$$\begin{aligned} \frac{4\pi}{c} \mathbf{J} &= \nabla \times \mathbf{B} \\ &= -\frac{dB_z}{dr} \mathbf{e}_\theta + \frac{1}{r} \frac{d}{dr} (r B_\theta) \mathbf{e}_z \end{aligned} \quad (39)$$

Using Eq. (39), the left-hand side of Eq. (37) is written as

$$\begin{aligned} \frac{4\pi}{c} \mathbf{J} \times \mathbf{B} &= \left(\frac{4\pi}{c} J_\theta B_z - \frac{4\pi}{c} J_z B_\theta \right) \mathbf{e}_r \\ &= \left(-\frac{dB_z}{dr} B_z - \frac{1}{r} \frac{d}{dr} (r B_\theta) B_\theta \right) \mathbf{e}_r. \end{aligned}$$

Then the force balance equation (37) is written as

$$-\frac{dB_z}{dr} B_z - \frac{1}{r} \frac{d}{dr} (r B_\theta) B_\theta = 4\pi \frac{dP}{dr}. \quad (40)$$

The profile of pressure P is assumed known to us (concrete forms of the pressure profile will be given later in this note, e.g., Eqs. (62) and (71)). Note that the force balance equation only give constraint on the perpendicular current density, the parallel current density still has some degree of freedom. To fix this freedom, we can specify either the radial profile of the parallel current density or the profile of the safety factor. Next, we will discuss these two cases.

4.1 Cylindrical equilibrium equation with given safety factor profile

The safety factor q in the cylindrical geometry is defined by

$$q(r) = \frac{B_z r}{B_\theta R}, \quad (41)$$

where R is an arbitrary constant with the dimension of length. Using Eq. (41), we obtain

$$B_z = \frac{q B_\theta R}{r}, \quad (42)$$

which can be used in the radial force balance equation (40) to eliminate B_z in favor of q , giving

$$\frac{d}{dr} \left(\frac{q B_\theta R}{r} \right) \frac{q B_\theta R}{r} + \frac{1}{r} \frac{d}{dr} (r B_\theta) B_\theta = -4\pi \frac{dP}{dr}. \quad (43)$$

The above equation can be arranged in the following form

$$\left[1 + \left(\frac{qR}{r} \right)^2 \right] B_\theta \frac{dB_\theta}{dr} + \frac{B_\theta^2}{r} \left[\frac{qR^2}{r} \frac{dq}{dr} - \left(\frac{qR}{r} \right)^2 + 1 \right] = -4\pi \frac{dP}{dr}, \quad (44)$$

which can be further written in the form that are convenient to be used in a numerical ODE integrator:

$$\frac{dB_\theta}{dr} = \left\{ -4\pi \frac{dP}{dr} - \frac{B_\theta^2}{r} \left[\frac{qR^2}{r} \frac{dq}{dr} - \left(\frac{qR}{r} \right)^2 + 1 \right] \right\} \left[1 + \left(\frac{qR}{r} \right)^2 \right]^{-1} \frac{1}{B_\theta} \quad (45)$$

4.1.1 Normalized equilibrium equations

Define $\bar{r} = r/a$, $\bar{B} = B/B_0$, $\bar{B}_z = B_z/B_0$, $\bar{B}_\theta = B_\theta/B_0$, $\bar{P} = P/[B_0^2/(8\pi)]$, where a is the minor radius of the device, B_0 is the value of B_z very near the magnetic axis, then Eq. (45) is written as

$$\frac{d\bar{B}_\theta}{d\bar{r}} = \left\{ -\frac{1}{2} \frac{d\bar{P}}{d\bar{r}} - \frac{\bar{B}_\theta^2}{\bar{r}} \left[\frac{q}{\varepsilon_a^2 \bar{r}} \frac{dq}{d\bar{r}} - \left(\frac{q}{\varepsilon_a \bar{r}} \right)^2 + 1 \right] \right\} \left[1 + \left(\frac{qR}{r} \right)^2 \right]^{-1} \frac{1}{\bar{B}_\theta}, \quad (46)$$

where $\varepsilon_a = a/R$. Equation (46) is used in my numerical code to advance B_θ from $\bar{r} = \bar{r}_0^+$ to $\bar{r} = 1$, where \bar{r}_0^+ is a small number ($\bar{r}_0^+ = 10^{-8}$). It is obvious that the initial condition of B_θ at \bar{r}_0^+ is

$$B_\theta(\bar{r}_0^+) = \frac{B_0 \bar{r}_0^+}{q(\bar{r}_0^+)} \varepsilon_a. \quad (47)$$

4.1.2 Numerical results

The safety factor profile is chosen as

$$q(\bar{r}) = 0.218833 - 0.406249 \bar{r}^2 + 0.268598 \bar{r}^4 - 0.163605 \bar{r}^6 + 0.092078 \bar{r}^8, \quad (48)$$

The profile of the pressure is chosen as

$$\bar{P}(\bar{r}) = a_0 \left(1.037632 + 0.517353 \bar{r}^2 - 6.776814 \bar{r}^4 + 7.683398 \bar{r}^6 - 2.466511 \bar{r}^8 + 3.5 e^{-\bar{r}^2/0.044} \right), \quad (49)$$

where a_0 in expression (49) is a normalizing factor, which is included to make $\bar{P} = 0.09$ at $\bar{r} = 0$ (i.e. to make $\beta(0) = 0.09$). It is ready to obtain $a_0 = 0.09/(1.037632 + 3.5)$.

[What we actually need is $d\bar{P}/d\bar{r}$, which can be calculated from the above formula to give

$$\frac{d\bar{P}}{d\bar{r}} = \left[2 \times 0.5173 \bar{r} - 4 \times 6.776 \bar{r}^3 + 6 \times 7.683 \bar{r}^5 - 8 \times 2.4665 \bar{r}^7 + 3.5 \exp\left(-\frac{\bar{r}^2}{0.044}\right) \times \left(-\frac{2\bar{r}}{0.044}\right) \right] \times \frac{0.09}{4.5376}, \quad (50)$$

]

Figure 7 plots the profile of B_θ and B_z , along with the profile of q and the pressure \bar{P} . (My numerical code is located at `/home/yj/project/cylindrical_q_solver/`.)

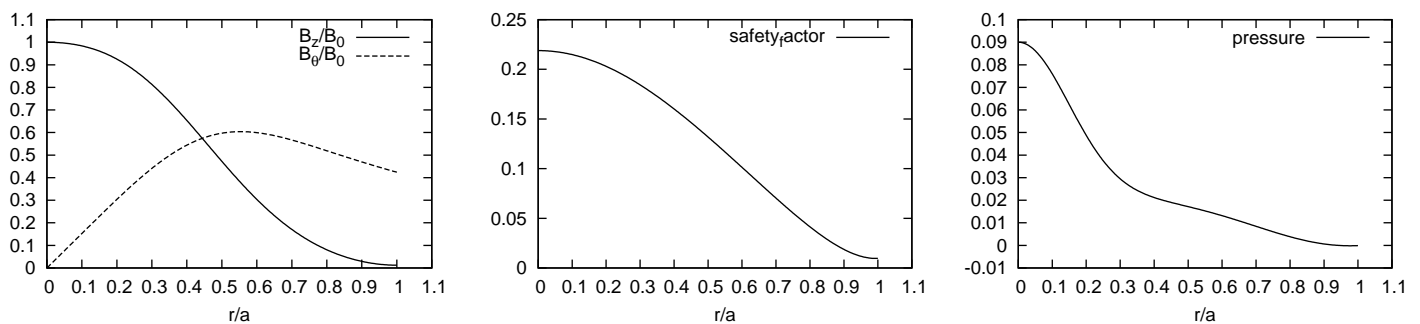


Figure 7. Equilibrium profile with $a/R = 1/3$. These results for B_z and B_θ agree with the analytical results given in Fig. 3 (there is minor discrepancy between B_θ at the locations $r/a \sim 1$, which may be due to the errors introduced by the interpolating formula used to obtaining the analytical expression).

It is mentioned in Huishan's notes that $d(B_\theta^2/\bar{r}^2)/d\bar{r}$ can be written analytically in the form

$$\frac{d}{d\bar{r}} \left(\frac{B_\theta^2}{\bar{r}^2} \right) = -\frac{2B_\theta^2}{\bar{r}^2 B^2} \left(4\pi \frac{dp}{d\bar{r}} + \frac{2B_\theta^2}{\bar{r}} + \frac{B_z^2}{q} \frac{dq}{d\bar{r}} \right), \quad (51)$$

which can be used to evaluate $d(B_\theta^2/\bar{r}^2)/d\bar{r}$ once the terms on the right-hand side is known. On the other hand we can also use directly the numerical results for B_θ to calculate the numerical derivative of B_θ^2/\bar{r}^2 with respect to \bar{r} . The results obtained by these two methods are compared in Fig. 8, which, as expected, show that they agree with each other.

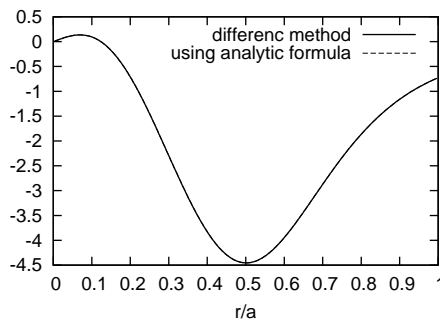


Figure 8. The results of $d(\bar{B}_\theta^2/\bar{r}^2)/d\bar{r}$ calculated by the two methods agree with each other very well (they agree with each other so well that they are indistinguishable in this scale). Here $\bar{B}_\theta \equiv B_\theta/B_0$.

4.2 Cylindrical equilibrium with parallel current density profile given

Define

$$\sigma(r) \equiv \frac{4\pi}{c} \frac{J_\parallel}{B}, \quad (52)$$

which represents the radial profile of the current density. On the other hand, the parallel current density can be written as

$$\begin{aligned} J_{\parallel} &= \frac{\mathbf{J} \cdot \mathbf{B}}{B} \\ &= [J_z(r)\mathbf{e}_z + J_{\theta}(r)\mathbf{e}_{\theta}] \cdot [B_z(r)\mathbf{e}_z + B_{\theta}(r)\mathbf{e}_{\theta}]/B \\ &= (J_z B_z + J_{\theta} B_{\theta})/B \\ &= \frac{c}{4\pi B} \frac{1}{r} \frac{d}{dr} (r B_{\theta}) B_z - \frac{c}{4\pi B} \frac{dB_z}{dr} B_{\theta} \end{aligned} \quad (53)$$

Using this, Eq. (52) is written as

$$\frac{1}{r} \frac{d}{dr} (r B_{\theta}) B_z - \frac{dB_z}{dr} B_{\theta} = B^2 \sigma. \quad (54)$$

Equations (40) and (54) are the governing equations for the equilibrium magnetic field. Combining Eqs. (40) and (54), we obtain

$$-\frac{dB_z}{dr} = \sigma B_{\theta} + 4\pi \frac{dP}{dr} \frac{B_z}{B^2}, \quad (55)$$

and

$$\frac{1}{r} \frac{d}{dr} (r B_{\theta}) = \sigma B_z - 4\pi \frac{dP}{dr} \frac{B_{\theta}}{B^2}, \quad (56)$$

which agree with the equations given in Huishan's notes.

4.2.1 Normalized equilibrium equations

Define $\bar{r} = r/a$, $\bar{B} = B/B_0$, $\bar{B}_z = B_z/B_0$, $\bar{B}_{\theta} = B_{\theta}/B_0$, $\bar{P} = P/[B_0^2/(8\pi)]$, where a is the minor radius of the device, B_0 is the value of B_z very near the magnetic axis, then Eqs. (55) and (56) are written respectively as

$$-\frac{d\bar{B}_z}{d\bar{r}} = \bar{\sigma} \bar{B}_{\theta} + \frac{1}{2} \frac{d\bar{P}}{d\bar{r}} \frac{\bar{B}_z}{\bar{B}^2}, \quad (57)$$

and

$$\frac{1}{\bar{r}} \frac{d}{d\bar{r}} (\bar{r} \bar{B}_{\theta}) = \bar{\sigma} \bar{B}_z - \frac{1}{2} \frac{d\bar{P}}{d\bar{r}} \frac{\bar{B}_{\theta}}{\bar{B}^2}, \quad (58)$$

where $\bar{\sigma}(r) \equiv a\sigma$. Equations (57) and (58) can be further written in forms that are convenient to be used in a numerical ODE integrator:

$$\frac{d\bar{B}_z}{d\bar{r}} = -\bar{\sigma} \bar{B}_{\theta} - \frac{1}{2} \frac{d\bar{P}}{d\bar{r}} \frac{\bar{B}_z}{\bar{B}^2}, \quad (59)$$

$$\frac{d\bar{B}_{\theta}}{d\bar{r}} = -\frac{1}{\bar{r}} \bar{B}_{\theta} + \bar{\sigma} \bar{B}_z - \frac{1}{2} \frac{d\bar{P}}{d\bar{r}} \frac{\bar{B}_{\theta}}{\bar{B}^2}, \quad (60)$$

My numerical code solving the above equations is at `/home/yj/project/cylindrical_j_solver`.

4.2.2 Reverse Field Pinch (RFP) equilibrium

Set the profile of the parallel current density as

$$\sigma(r) = \frac{2\Theta_0}{a} \left[1 - \left(\frac{r}{a} \right)^{\alpha} \right], \quad (61)$$

where α and Θ_0 are constants, and the pressure profile as

$$4\pi \frac{dP}{dr} = -\chi(r) \frac{r}{2} \left(\frac{\sigma B^2}{2B_{\theta}} - \frac{B_z}{r} \right)^2, \quad (62)$$

where $\chi(r)$ is a given dimensionless function. (The profiles are specified in Huishan's notes). Next, we specify the "initial condition" of Eqs. (55) and (56). We set the value of B_z at the location $r = r_0^+$:

$$B_z(r_0^+) = B_0, \quad (63)$$

where B_0 is a known constant, and r_0^+ is an infinitesimal, i.e., $r_0^+ \rightarrow 0^+$ (in the numerical code, the small quantity \bar{r}_0^+ is set as $\bar{r}_0^+ = 10^{-5}$). Then, according to the definition of the safety factor, the poloidal field at r_0^+ is written as

$$B_{\theta}(r_0^+) = \frac{B_0 r_0^+}{q(r_0^+) R}. \quad (64)$$

As mentioned in Huishan's notes, the safety factor at r_0^+ is fixed to

$$q(r_0^+) = \frac{a}{R\Theta_0}. \quad (65)$$

Using this, Eq. (64) is written as

$$B_{\theta}(r_0^+) = B_0 \Theta_0 \frac{r_0^+}{a}. \quad (66)$$

Equations (63) and (66) provide the “initial condition” to determine the solution of Eqs. (55) and (56). In the normalization specified in Sec. 4.2.1, Eq. (63) and (66) are written as

$$\bar{B}_z(\bar{r}_0^+) = 1, \quad (67)$$

$$\bar{B}_\theta(\bar{r}_0^+) = \Theta_0 \bar{r}_0^+. \quad (68)$$

In the normalization, the profiles in Eqs. (61) and (62) are written as

$$\bar{\sigma}(\bar{r}) = 2\Theta_0[1 - \bar{r}^\alpha] \quad (69)$$

$$g(\bar{r}) = -\chi(\bar{r}) \frac{\bar{r}}{2} \left(\frac{\bar{\sigma} \bar{B}^2}{2\bar{B}_\theta} - \frac{1}{\bar{r}} \bar{B}_z \right)^2. \quad (70)$$

Figure 9 plots the profiles of equilibrium magnetic field, safety factor, and thermal pressure.

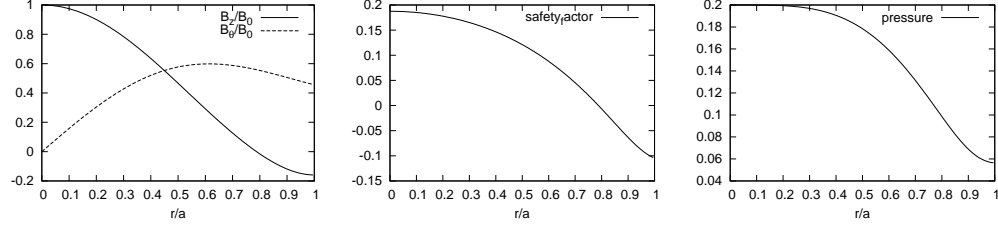


Figure 9. (a) Profile of the magnetic field obtained for the parameters $\chi = 1.0$, $\alpha = 5.5$, and $\Theta_0 = 1.6$. (b) Profile of safety factor obtained with parameter $a/R = 0.3$. (c) Pressure profile (normalized by $B_0^2/(8\pi)$) for parameter $\beta(0) = 0.2$, where $\beta(0) \equiv P_0/(B_0^2/8\pi)$ is the ratio of thermal pressure to magnetic pressure at the magnetic axis.

4.2.3 Another RFP equilibrium

An RFP equilibrium slightly different from the above is used in one of Huishan’s notes. Since I was asked to repeat his calculation to verify his numerical results, I need to use the same equilibrium as he used. The RFP equilibrium is different from that in the above subsection in that $\bar{\sigma}$ and \bar{P} are chosen as follows:

$$\bar{\sigma} = \frac{2\varepsilon_a}{q(0)}[1 - \bar{r}^\alpha],$$

$$\bar{P} = a_0 \left(1.037632 + 0.517353 \bar{r}^2 - 6.776814 \bar{r}^4 + 7.683398 \bar{r}^6 - 2.466511 \bar{r}^8 + 3.5e^{-\bar{r}^2/0.044} \right), \quad (71)$$

where $q(0) = 0.2188$, $\varepsilon_a = 0.5/1.5$, $\alpha = 5.5$, $a_0 = 0.09/(1.037632 + 3.5)$.

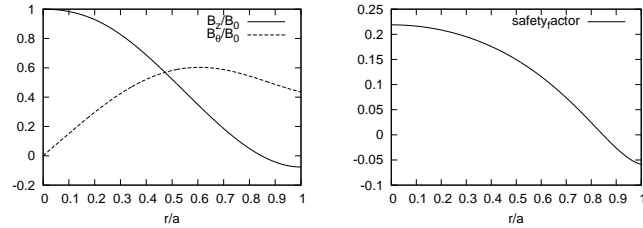


Figure 10. Profile of the magnetic field (a) and safety factor (b).

The equation I was asked to solve is given by (refer to Huishan’s notes)

$$\frac{d^2\chi}{dr^2} - \chi \left[-\frac{m^4 + 10m^2n^2\varepsilon^2 - 3n^4\varepsilon^4}{4r^2(m^2 + n^2\varepsilon^2)^2} + \frac{m^2 + n^2\varepsilon^2}{r^2} - \sigma^2 + \frac{2n\varepsilon(m\sigma + n\varepsilon g)}{r(m^2 + n^2\varepsilon^2)} \right] = \frac{\chi}{F} \left[G \frac{d\sigma}{dr} - \frac{d(gF)}{dr} + \frac{2mn\varepsilon Gg}{r(m^2 + n^2\varepsilon^2)} - G\sigma g \right], \quad (72)$$

where $F = mB_\theta - n\varepsilon B_z$, $G = mB_z + n\varepsilon B_\theta$, $\varepsilon = r/R$, $g = d\bar{P}/dr$. Equation (72) can be rewritten as

$$\frac{d^2\chi}{d\bar{r}^2} - \chi \left[-\frac{m^4 + 10m^2n^2\varepsilon_a^2\bar{r}^2 - 3n^4\varepsilon_a^4\bar{r}^4}{4\bar{r}^2(m^2 + n^2\varepsilon_a^2\bar{r}^2)^2} + \frac{m^2 + n^2\varepsilon_a^2\bar{r}^2}{\bar{r}^2} - \bar{\sigma}^2 + \frac{2n\varepsilon_a\bar{r}(m\bar{\sigma} + n\varepsilon_a\bar{r}\bar{g})}{\bar{r}(m^2 + n^2\varepsilon_a^2\bar{r}^2)} \right] = \frac{\chi}{F} \left[G \frac{d\bar{\sigma}}{d\bar{r}} - \frac{d(\bar{g}F)}{d\bar{r}} + \frac{2mn\varepsilon_a\bar{r}G\bar{g}}{\bar{r}(m^2 + n^2\varepsilon_a^2\bar{r}^2)} - G\bar{\sigma}\bar{g} \right], \quad (73)$$

where $\bar{g} = d\bar{P}/d\bar{r}$.

5 Numerical results of eigenmodes—to be deleted

In this section, uniform density profile is assumed. We first consider the case of mode number $m = 1$ and $n = 1$. Figs. 11, 12, and 13 plot continuum spectrum and eigenfunction of continuum mode with mode frequency lying in the continuum spectrum.

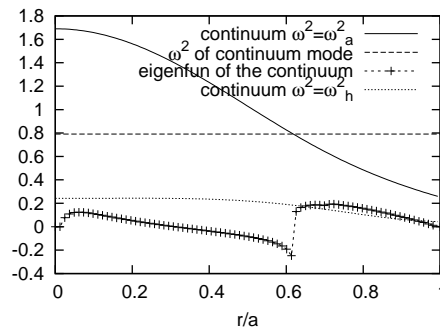


Figure 11. (wrong!!) Continuum spectrum $\omega^2 = \omega_a^2$ and $\omega^2 = \omega_b^2$. The eigenfunction of a continuum mode with frequency $\omega^2 = 0.79087$ is also plotted. Note that the eigenfunction has singularity at the location where its frequency intersects with the $\omega^2 = \omega_a^2$ continuum spectrum.

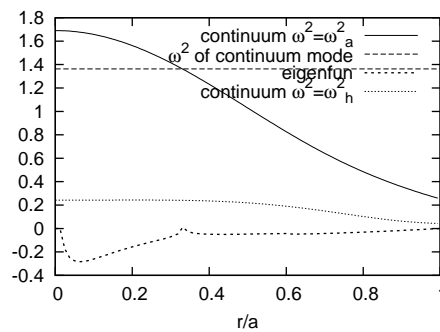


Figure 12. (wrong!!) Continuum spectrum $\omega^2 = \omega_a^2$ and $\omega^2 = \omega_b^2$. The eigenfunction of a continuum mode with frequency $\omega^2 = 1.36234$ is also plotted. Note that the eigenfunction has singularity (not obvious in this case) at the location where its frequency intersects with the $\omega^2 = \omega_a^2$ continuum spectrum.

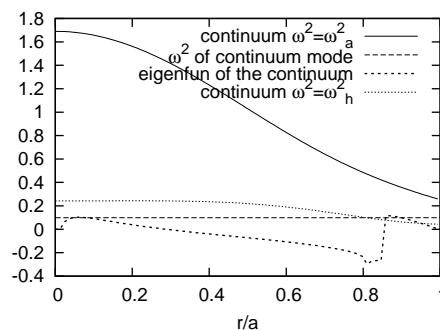


Figure 13. (wrong!!) Continuum spectrum $\omega^2 = \omega_a^2$ and $\omega^2 = \omega_b^2$. The eigenfunction of a continuum mode with frequency $\omega^2 = 0.0988$ is also plotted. Note that the eigenfunction has singularity at the location where its frequency intersects with the $\omega^2 = \omega_b^2$ continuum spectrum.

Fig. 14 plots the frequency and mode structure of a global mode.

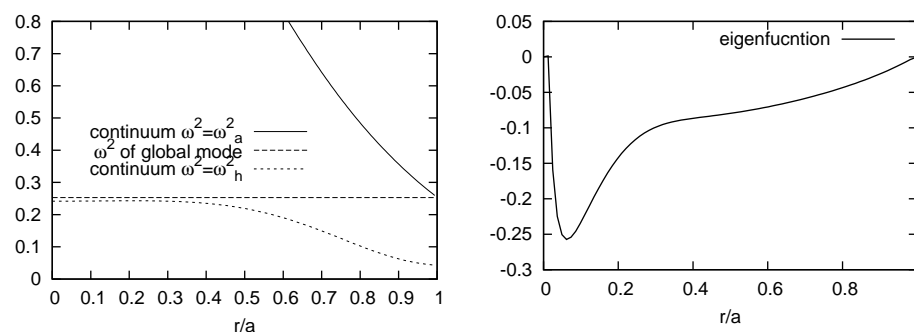


Figure 14. (wrong!!) Left figure: Frequency gap between the continuum spectrum $\omega^2 = \omega_a^2$ and $\omega^2 = \omega_b^2$. Right figure: The eigenfunction of a global mode with frequency $\omega^2 = 0.2530$ lying in the frequency gap (this frequency is indicated in the left figure).

Next consider the case of $m = 1$ and $n = 5$.

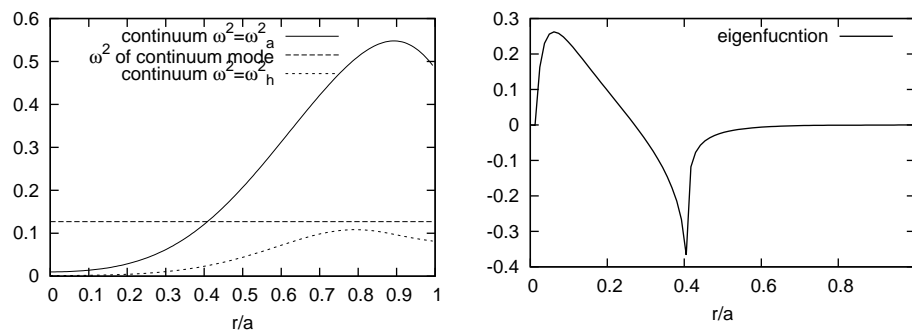


Figure 15. (wrong!) Left figure: Continuum spectrum $\omega^2 = \omega_a^2$ and $\omega^2 = \omega_h^2$. Right figure: The eigenfunction of a mode with frequency $\omega^2 = 0.126907$ (this frequency is indicated in the left figure).

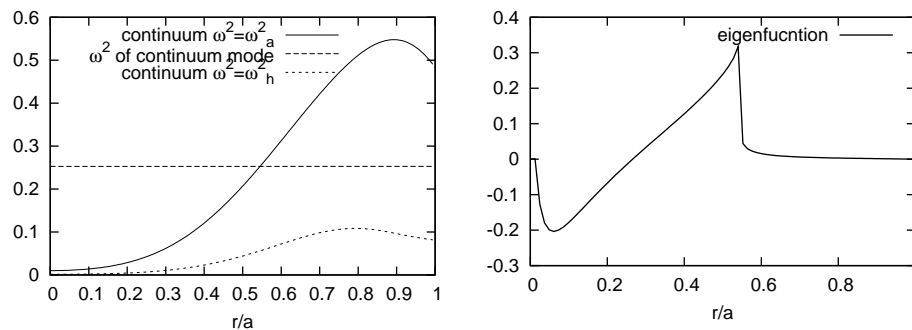


Figure 16. (wrong!) Left figure: Continuum spectrum $\omega^2 = \omega_a^2$ and $\omega^2 = \omega_h^2$. Right figure: The eigenfunction of a continuum mode with frequency $\omega^2 = 0.252936$ (this frequency is indicated in the left figure).

Examining the above two figures, we find that the continuum spectrum $\omega^2 = \omega_a^2$ and $\omega^2 = \omega_h^2$ for this case does not have “gap” structure. Note that the continuum $\omega^2 = \omega_h^2$ has an minimum in the vicinity of $r/a \sim 0$. As mentioned in many papers, a global mode, whose frequency is just below the minimum of the continuum spectrum, may exist. Figure 8 plots a global mode of this kind.

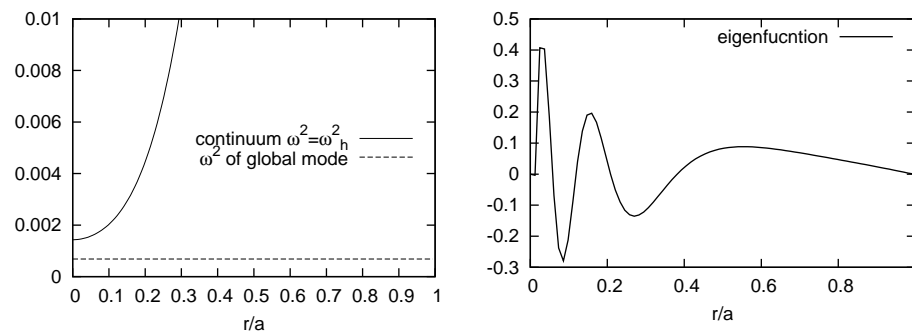


Figure 17. (wrong!) Left figure: Continuum spectrum $\omega^2 = \omega_h^2$. Right figure: The eigenfunction of a global mode with frequency $\omega^2 = 6.8263 \times 10^{-4}$ lying under the extremum of the Alfvén continuum $\omega^2 = \omega_h^2$. (this frequency is indicated in the left figure).

Bibliography

- [1] Limin Yu, Guo yong Fu, and Zheng-Mao Sheng. Kinetic damping of alfvén eigenmodes in general tokamak geometry. *Physics of Plasmas*, 16(7):072505, 2009.